





RESEARCH ARTICLE | FEBRUARY 15 2022

Artificial synapses based on Josephson junctions with Fe nanoclusters in the amorphous Ge barrier ^F

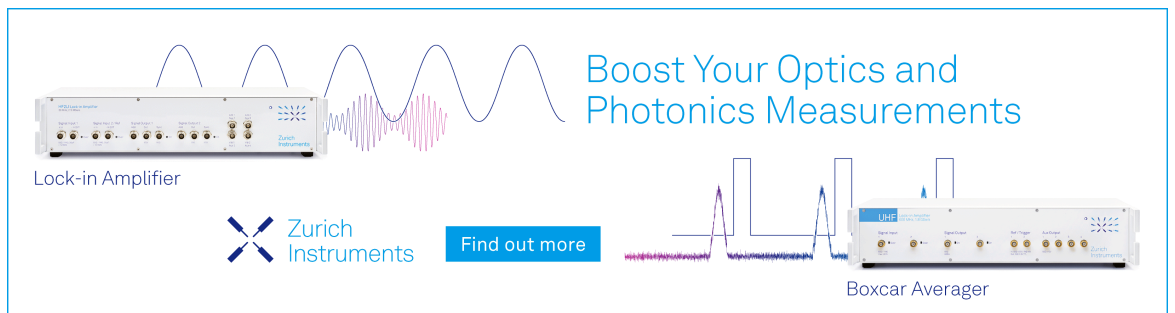
Emilie Jué ; Gleb Iankevich; Thomas Reisinger; Horst Hahn ; Virgil Provenzano; Matthew R. Pufall; Ian W. Haygood ; William H. Rippard; Michael L. Schneider 



J. Appl. Phys. 131, 073902 (2022)
<https://doi.org/10.1063/5.0080841>



CrossMark



Boost Your Optics and Photonics Measurements

Lock-in Amplifier

Zurich Instruments

Find out more

Boxcar Averager

Artificial synapses based on Josephson junctions with Fe nanoclusters in the amorphous Ge barrier



Cite as: J. Appl. Phys. 131, 073902 (2022); doi: 10.1063/5.0080841

Submitted: 3 December 2021 · Accepted: 21 January 2022 ·

Published Online: 15 February 2022



Emilie Jué,^{1,2,a)} Gleb Iankevich,^{3,4} Thomas Reisinger,^{3,4} Horst Hahn,^{3,4} Virgil Provenzano,^{4,5} Matthew R. Pufall,⁶ Ian W. Haygood,^{1,2} William H. Rippard,⁶ and Michael L. Schneider⁶

AFFILIATIONS

¹Department of Physics, University of Colorado Boulder, Boulder, Colorado 80309, USA

²Associate of the National Institute of Standards and Technology, Boulder, Colorado 80305, USA

³Institute for Quantum Materials and Technologies, Karlsruhe Institute of Technology, 76344 Eggenstein-Leopoldshafen, Germany

⁴Institute of Nanotechnology, Karlsruhe Institute of Technology, 76344 Eggenstein-Leopoldshafen, Germany

⁵Materials Science and Engineering Division, National Institute of Standards and Technology, Gaithersburg, Maryland 20899, USA

⁶Quantum Electromagnetics Division, National Institute of Standards and Technology, Boulder, Colorado 80305, USA

^{a)}Author to whom correspondence should be addressed: emilie.jue@nist.gov

ABSTRACT

We have measured the synaptic properties of a magnetic Josephson junction (MJJ) consisting of a barrier of amorphous Ge containing size-selected Fe nanoclusters between two Nb electrodes. We show that the critical current of the device varies with the magnetic order of the clusters and that the magnetic order can be tuned in a quasi-analog way with short electrical pulses of 16 pJ applied through the device. This is the first demonstration of critical current tuning via magnetic order in a nano-clustered MJJ in a material system other than SiMn. This result eliminates the need for a postdeposition annealing step for synaptic MJJs in neuromorphic applications and opens new options to optimize materials, which has the potential to improve the performance of the MJJs and provide a better understanding of the physics of the device.

Published under an exclusive license by AIP Publishing. <https://doi.org/10.1063/5.0080841>

I. INTRODUCTION

Over the last decade, superconducting electronics for neuromorphic applications have shown substantial progress in terms of devices, circuits, and architectures.¹ Superconducting electronics has many advantages for neuromorphic computing, including Josephson junctions whose natural spiking behavior can mimic the action potential fired in the brain by the neurons.^{2,3} These inherent spiking properties enable superconducting spiking neural networks⁴ that can be high speed and energy efficient in applications, such as pattern recognition and signal detection.^{5–10} One important element that is found in neural networks is the synapse, which can vary the connection strength between two neurons and is responsible for the plasticity in the brain. In superconducting electronics, it has been shown that synaptic properties can be obtained with nano-clustered magnetic Josephson junctions (MJJs).¹¹

A nano-clustered MJJ is a hybrid magnetic-superconducting device that can be used as an artificial synapse for neuromorphic

circuits. It consists of a Josephson junction with a non-superconducting barrier that contains magnetic clusters. The magnetic order of the nanoclusters in this type of MJJ can be used to change the critical current of the Josephson junction, which can be used to implement the synaptic weight function.¹² Despite their promising performance in terms of energy and speed, the synaptic behavior of nanocluster-based MJJs has been demonstrated in only one material system so far: an Si barrier with Mn nanoclusters between two electrodes of Nb.¹¹ It is known from work on thin-film MJJs^{13–19} that different magnetic materials in a hybrid magnetic-superconducting system can have a significant impact on the critical current (I_C) of the device.^{18,20,21} Thus, it is important to measure the I_C impact of different materials on nano-clustered MJJs. Demonstrating nano-clustered MJJs, using other material systems, would provide new options to optimize materials for synaptic MJJs in neuromorphic applications to tune the device performance and to better understand the physics involved in the device.

21 March 2024 10:01:35

For example, being able to increase the $I_C R_N$ factor, where R_N is the normal state resistance of the device, will improve the speed of the device.²² Reducing the size and the magnetic moment of the nanoclusters could enable a reduction in the energy required to train the device, i.e., the energy required to order or disorder the magnetic clusters constituting the MJJ. Working with a material that does not need a high temperature anneal (such as 400 °C as required with SiMn MJJs¹¹) would also allow the integration of the device in more superconducting circuits.^{23,24}

In this work, we show that we can reproduce the synaptic properties of the MJJ in a new material system that consists of a barrier of amorphous Ge containing Fe nanoclusters between two Nb electrodes. Using a method of field cooling, we show that the critical current in the GeFe MJJ depends on the magnetic order of the clusters. Finally, we demonstrate that the variation of the critical current can be tuned in a quasi-analog way with short electrical pulses of 16 pJ, which is comparable to the previous observation made in the SiMn system. These results show that the synaptic properties of the MJJ are not limited to the SiMn system and are thus encouraging for the exploration of new material systems for synaptic devices in superconducting neuromorphic applications.

II. DEVICES, EXPERIMENTAL SETUP, AND METHOD

The sample used for this study is composed of Nb(100)/Ge_mFe_x (6.2)/Nb(20), where the numbers in parentheses are the thickness in nanometers and the notation Ge_mFe_x stands for nanoclusters of iron in a matrix of germanium. The barrier of GeFe was grown with a custom-made deposition system, which allows the deposition of size-selected nanoparticles (clusters) at low impact energies.^{25,26} The Nb films were deposited in a separate electron-beam evaporation system, to which the sample was transferred in ultrahigh vacuum. Note that another 100 nm of Nb was deposited on top of the sample during the processing to make the top electrode and the wiring layer. The nanoclusters are selected to have a size of 1000 ± 100 atoms of Fe per cluster (corresponding to diameters of 2.9 ± 0.1 nm), and their concentration in the barrier is approximately 17 vol. % assuming bulk density of iron for the nanoclusters. The nanoclusters clusters are superparamagnetic, meaning that the magnetization of the cluster is monodomain and its direction is blocked in a given direction when the temperature is below a characteristic value called the blocking temperature (T_B). Here, the average blocking temperature of the magnetic clusters is measured to be 40 ± 5 K, which was determined from field-cooling measurements similar to the ones described below.

A schematic circuit of the experimental setup is shown in Fig. 1. The sample is patterned into $8 \mu\text{m}$ -diameter circular MJJ devices using optical lithography. These devices are measured in a cryogenic probe station with a base temperature of 4 K. A 93 Hz triangular waveform is applied to the device via ground-signal-ground probes. The triangular waveform input and the amplified output voltages are sent to an oscilloscope to measure the characteristic current-voltage (I - V) curve of the junction. Finally, nanosecond electrical pulses can be applied through the device to modify the magnetic order of the MJJ as described in the method below.

The magnetic order of the device is defined by the average orientation of the nanoclusters' magnetization within the device: a

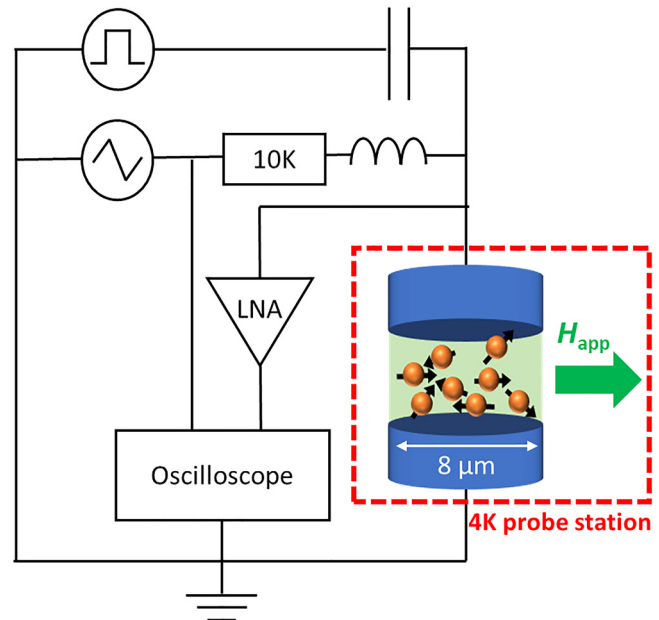


FIG. 1. Schematic circuit of the experimental setup. A bias tee is used to separate the slow 93 Hz-triangular waveform needed to measure the superconducting properties of the device and the fast-electrical pulses used to modify the magnetic order of the MJJ. The sample is placed inside a temperature-variable cryogenic probe operated at 4 K. An external magnetic field (H_{app}) inside the cryostat is used to modify the magnetic order of the clusters (see Sec. II). To measure the characteristic I - V curve of the junction, the output signal from the device amplified with a low noise amplifier (LNA) and the triangular waveform input are both sent to an oscilloscope.

21 March 2024 10:01:35

disordered magnetic state is obtained when the magnetization of the clusters points in random directions, whereas a highly ordered magnetic state is obtained when the magnetization of the clusters is aligned in a given direction. The methods used in this work to control the magnetic order of the clusters are described in Fig. 2. The disordered magnetic state is obtained with a method of zero field cooling (ZFC), which consists of heating the device above its blocking temperature ($T_B \approx 40$ K) and then cooling the device in the absence of a magnetic field [Fig. 2(a)]. To increase the magnetic order of the junction, we use two different methods. A fully or partially ordered state can be obtained with a field-cooling (FC) method, where the device is heated up to a given temperature T_{max} and then cooled down in the presence of a magnetic field [Fig. 2(b)]. The higher the maximum temperature (with $T_{\text{max}} < T_B$) and the magnetic field, the higher the magnetic order. Although this method is easy to implement, it is slow and not desirable for neuromorphic applications due to the need to vary the temperature. Another way to control the magnetic order of the device is to use field-assisted electrical pulse control. This method has the advantage of being fast, and the magnetic order can be controlled while maintaining a 4 K temperature. In this case, a magnetically ordered junction is obtained by applying electrical pulses in the presence of a magnetic field [Fig. 2(c)]. The degree of order depends on the pulse parameters and on the

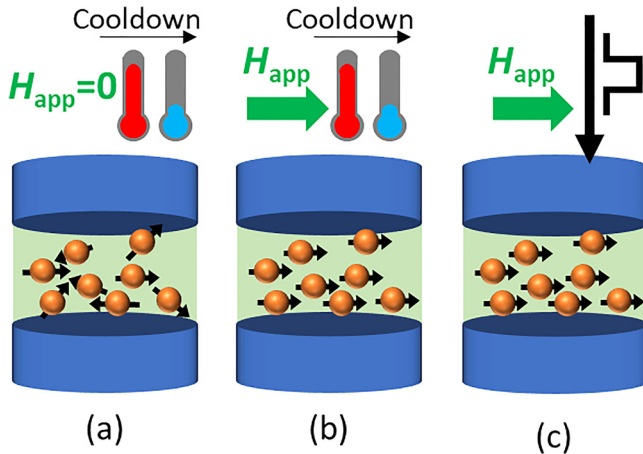


FIG. 2. The magnetic order of the device is controlled with three different methods: (a) Disordering with zero field cooling (ZFC), (b) ordering with field cooling (FC), and (c) ordering with field-assisted electrical pulse control. See the main text for a detailed description of the three methods.

value of the magnetic field. For this experiment, we typically used repetitions of 10 ns pulses of 280 ± 10 mV, which, as described further, corresponds to a pulse energy of 16 pJ.

Finally, any major changes, such as contacting a device, applying electrical pulses, or ramping the magnetic field can generate trapped flux due to persistent current loops that can distort the measurement. To remove any potential trapped flux, a defluxing procedure is performed after each major change. Defluxing consists of heating the system above the superconducting critical temperature of the junctions and Nb wiring ($T_C \approx 9$ K) and then returning to 4 K before measurements. We note that the defluxing method would not be energy and time efficient for neuromorphic applications if it is needed frequently, e.g., after each training pulse sequence. However, a previous study with SiMn demonstrated that using current pulses with energies no larger than 100 pJ and limiting the magnetic field (to 20 mT) does not generate trapped flux,¹¹ meaning that both training and inference could potentially be done without the need for the defluxing of the circuit.

III. RESULTS

One requirement for an MJJ to act as a synaptic device is that the critical current of the junction must be tunable with the magnetic ordering of the clusters. We study this property for the junctions with GeFe clusters using the ZFC and FC methods to control the magnetic order. Figure 3 shows the characteristic current-voltage (I - V) curves of the junction when the nanoclusters are disordered with ZFC and ordered with FC at 80 mT at a maximum temperature of 25 K. The measurements show a clear reduction of the critical current when the nanoclusters are ordered magnetically, confirming that the critical current is dependent on the magnetic order.

The data are fit with the Ivanchenko and Zil'berman (IZ) model,^{27,28} which accounts for the thermal noise responsible for

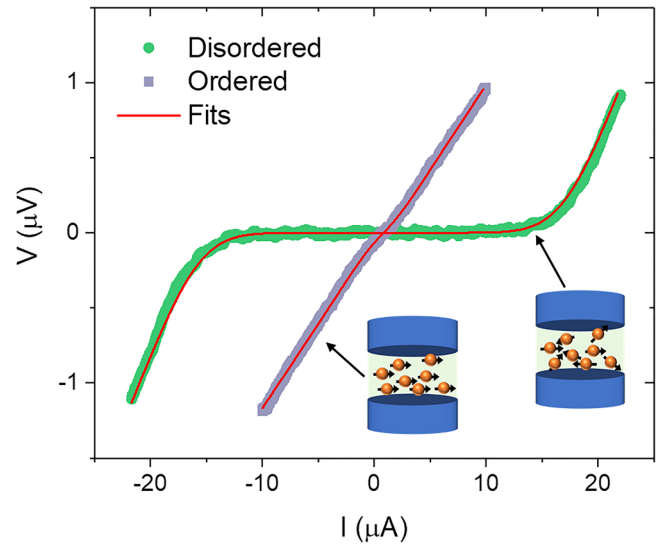


FIG. 3. Characteristic I - V curve of the MJJ measured at 4 K for two different magnetic orders. The disordered state (green) is obtained with zero field cooling, while the ordered state (purple) is obtained with a field cooling at 80 mT and a maximum temperature of 25 K. The data are fitted (red curves) with the Ivanchenko and Zil'berman model that takes into account the thermal noise in the measurement system.

the rounding of the curves near I_C and allows the extraction of the critical current I_C and the normal state resistance R_N of the device. The IZ model is described by the expression

$$V(I_C, R_N, T_{eff}) = I_C R_N \left(\frac{I}{I_C} - \mathcal{I}_- + \mathcal{I}_+ \right) \text{ for } I > 0, \quad (1)$$

where $\mathcal{I}_\pm = \frac{\mathcal{I}_{1 \pm i\nu}(\gamma_c)}{2i\mathcal{I}_{\pm i\nu}(\gamma_c)}$, $\gamma = \frac{I\hbar}{2ek_B T_{eff}}$, and $\gamma_c = \frac{I_C \hbar}{2ek_B T_{eff}}$. Here, $\mathcal{I}_\nu(z)$ is a modified Bessel function of the first kind with ν being a non-integer complex number, T_{eff} is the effective noise temperature in the measurement system, \hbar is the reduced Planck constant, e is the elementary charge, and k_B is the Boltzmann constant. The fits shown in Fig. 3 correspond to a normal state resistance of 112 ± 5 m Ω and a critical current of 27.0 ± 0.4 μ A or 2.0 ± 1.8 μ A when the junction is, respectively, magnetically disordered or ordered. The effective noise temperature is found to be 49 ± 4 K. Here, the uncertainty on R_N , T_{eff} , and I_C is determined by the standard deviation of the fitted values for 20 repetitions of the measurement of the I - V curves for both FC and ZFC. This same uncertainty in the critical current for FC and ZFC is shown by the error bars in Figs. 4 and 5. We note that there is a larger error bar that results from this averaging process for the FC measurements of I_C , compared to that for the ZFC measurements of I_C , as seen in Fig. 4.

We then study the influence on the device critical current due to the magnetic field strength during field cooling. The I_C measurements are repeated by alternating ZFC and FC, where the FC is performed with different values of the magnetic field and for a maximum temperature of 43 K. The I - V curve is measured after

21 March 2024 10:01:35

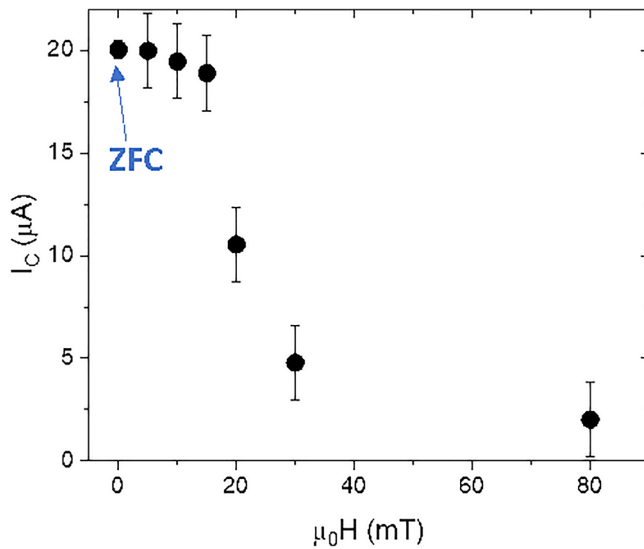


FIG. 4. Critical current as a function of the magnetic field during the FC ordering. The value for zero magnetic field corresponds to the critical current obtained after the ZFC disordering. Here, the ZFC is performed before each measurement of FC to reset the magnetic clusters to a disordered state. The error bar is defined by the standard deviation obtained for 20 measurements of ZFC and FC in the same conditions ($\Delta I_{C_ZFC} = 0.4 \mu\text{A}$ and $\Delta I_{C_FC} = 1.8 \mu\text{A}$).

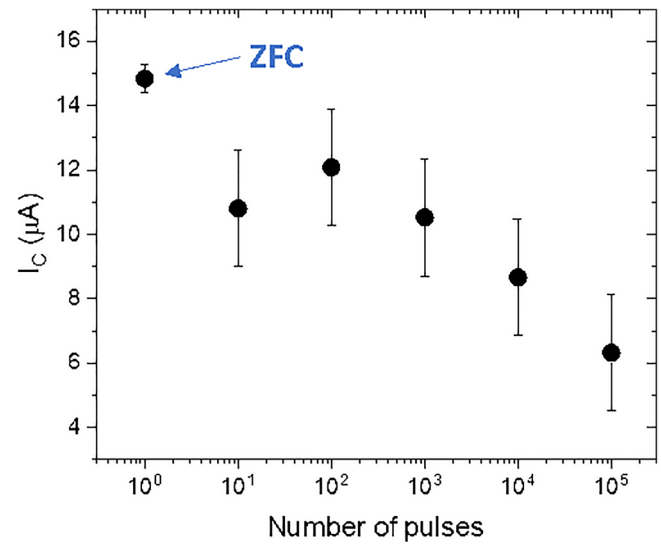


FIG. 5. Critical current as a function of the number of pulses applied through the junction in the presence of a magnetic field of 30 mT. The pulses are 10 ns long and have an amplitude of 280 ± 10 mV. The data point at 10^0 pulse corresponds to the critical current for the disordered state of the device obtained with the ZFC disordering method. Here, the ZFC is performed before each measurement of FC to reset the magnetic clusters to a disordered state. The error bar is defined by the standard deviation obtained for 20 measurements of ZFC and FC in the same conditions ($\Delta I_{C_ZFC} = 0.4 \mu\text{A}$ and $\Delta I_{C_FC} = 1.8 \mu\text{A}$).

each FC measurement, and the critical current is reported as a function of the magnetic field strength, as shown in Fig. 4. We observe intermediate values of critical current that correspond to intermediate ordering of the magnetic clusters between fully disordered and fully ordered. This result is important for neuromorphic applications since the intermediate values of critical current are required to tune the weight of the synaptic device.

Subsequently, we study the critical current of the device when the magnetic order is controlled with the field-assisted electrical pulse method. For that, we measure the characteristic I - V curves of the junction after the clusters have been ordered in the presence of a magnetic field of 30 mT with a certain number of 10 ns pulses of an amplitude of 280 ± 10 mV. Here, the pulse is measured with a high-speed oscilloscope, and its voltage amplitude is estimated at the sample after accounting for the measured input cabling and component losses. Assuming a 50Ω characteristic impedance of the cabling, the estimated energy of the pulse is 16 pJ. Considering the resistance of 112 ± 5 m Ω of our device, most of the energy is reflected due to the poor impedance match between the junction and the 50Ω lines. Using a DC analysis, the energy of the pulse dissipated in the MJJ, E_{pulse} , is estimated to be 35 fJ.

The critical current is extracted by fitting the I - V curves and is shown in Fig. 5 as a function of the number of pulses. Before each measurement, the device is magnetically disordered with the ZFC method. The general trend of the curve shows that the critical current decreases with the number of pulses with a reduction of the critical current by a factor of 2.3 after 10^5 pulses compared to the disordered state value. This result is similar to the reduction of

I_C with the number of electrical pulses previously observed in SiMn. Compared to the FC method, the current pulse method is faster for controlling and fine-tuning the magnetic order and the critical current of the device. This is a significant advantage for neuromorphic applications.

For neuromorphic applications, modifying the critical current from a high to low value can be used to strengthen or weaken the synapse depending on how it is integrated in the circuit. Since both actions are needed in a neural network, the critical current should ideally be modified with pulses in a reversible way. This capability was demonstrated in our previous work with SiMn:¹¹ the critical current can be reset to its highest value (magnetically disordered MJJ) by applying a current pulse in the absence of a magnetic field. Although this property was not the focus of our present study, we were able to make similar observations in GeFe. Further study is needed to more extensively characterize the ability to modify the critical current incrementally in both directions.

Finally, we note that the mechanism behind the ordering of the clusters with electrical pulses is not well understood. It seems unlikely that this mechanism can be attributed solely to thermal effects for the following reason. We estimate the temperature increase ΔT generated in the device when an electrical pulse is flowing through the MJJ with the following equation:

$$\Delta T = \frac{E_{pulse}}{m_{Ge}c_{Ge} + m_{Fe}c_{Fe}}, \quad (2)$$

where E_{pulse} is the pulse energy, $m_{\text{Ge,Fe}}$ is the mass of Ge or Fe inside the barrier ($m_{\text{Ge}} = 1.38$ pg and $m_{\text{Fe}} = 0.28$ pg), and $c_{\text{Ge,Fe}}$ is the specific heat capacity of Ge or Fe ($c_{\text{Ge}} = 0.32$ J g⁻¹ K⁻¹ and $c_{\text{Fe}} = 0.449$ J g⁻¹ K⁻¹). The mass of Ge and Fe in the barrier is obtained with the dimensions of the barrier, the concentration of clusters in the barrier, and the density of the materials ($\rho_{\text{Ge}} = 5.323$ g/cm³ and $\rho_{\text{Fe}} = 7.874$ g/cm³). Using the equation above, we estimate that the 35 fJ of energy dissipated by the electrical pulse through the MJJ gives rise to a temperature increase of $\Delta T \approx 56$ mK through the device. This value is three orders of magnitude below the blocking temperature of 40 ± 5 K for this device, which suggests that the pulse-induced magnetic ordering mechanism is unlikely to be attributable to thermal effects. Note that even considering a worst-case estimate that ignores any cooling processes and assumes that all the energy in the pulse (16 pJ) is absorbed by the barrier, the temperature through the device would increase only by $\Delta T \approx 25$ K, which is still below the blocking temperature of the device and is insufficient to modify the magnetic orientation of the clusters by thermal effects. More study of the transport is needed to explain this mechanism.

IV. SUMMARY

In summary, we have shown that nano-clustered GeFe MJJs could be used as artificial synapses in superconducting neuromorphic circuits. The critical behaviors that have been demonstrated in this study are that the critical current can be varied with the magnetic order of the clusters; intermediate values of critical current can be obtained with intermediate magnetic states between the fully ordered and the fully disordered state; these intermediate values can be reached with fast current pulses applied through the device. As far as the authors are aware, this is the first time that this behavior has been observed in a system other than in nano-clustered SiMn MJJs. Contrary to the SiMn barriers, the GeFe is deposited with a size-selective nanoparticle deposition system, which enables fine-tuning of the nano-cluster properties. This will allow more extensive studies on the properties of the device as a function of the parameters of the interlayer nano-composite in the junction (cluster size, cluster concentration, etc.). This has the potential to improve the performance of the devices (e.g., speed, energy efficiency, number of intermediate values of I_C accessible, etc.) as well as to help determine the physics of the device (e.g., transport properties, interaction between clusters, mechanism related to the pulse-induced magnetic ordering, etc.). Finally, the results of this study open up new options to explore and optimize materials for nano-clustered MJJ synaptic devices.

SUPPLEMENTARY MATERIAL

See the [supplementary material](#) for a more detailed description of the material deposition method.

ACKNOWLEDGMENTS

E.J. and I.W.H. acknowledge support under Cooperative Research Agreement Award No. 70NANB18H006 through the University of Colorado Boulder. H.H. acknowledges the financial support by the State of Hesse for the cluster-ion beam deposition

system used for the preparation of the samples. T.R., G.I., and H.H. are grateful for the support provided by the Program NACIP and MSE of the Helmholtz Association.

AUTHOR DECLARATIONS

Conflict of Interest

The authors have no conflicts to disclose.

DATA AVAILABILITY

Data available on request from the authors.

REFERENCES

- ¹M. L. Schneider, C. A. Donnelly, and S. E. Russek, "Tutorial: High-speed low-power neuromorphic systems based on magnetic Josephson junctions," *J. Appl. Phys.* **124**, 161102 (2018).
- ²P. Crotty, D. Schult, and K. Segall, "Josephson junction simulation of neurons," *Phys. Rev. E* **82**, 011914 (2010).
- ³K. Segall, M. Legro, S. Kaplan, O. Svitelskiy, S. Khadka, P. Crotty, and D. Schult, "Synchronization dynamics on the picosecond time scale in coupled Josephson junction neurons," *Phys. Rev. E* **95**, 032220 (2017).
- ⁴W. Maass, "Networks of spiking neurons: The third generation of neural network models," *Neural Netw.* **10**, 1659–1671 (1997).
- ⁵Y. Yamanashi, K. Umeda, and N. Yoshikawa, "Pseudo sigmoid function generator for a superconductive neural network," *IEEE Trans. Appl. Supercond.* **23**, 1701004 (2013).
- ⁶F. Chiarello, P. Carelli, M. G. Castellano, and G. Torrioli, "Artificial neural network based on SQUIDS: Demonstration of network training and operation," *Supercond. Sci. Technol.* **26**, 125009 (2013).
- ⁷A. E. Schegolev, N. V. Klenov, I. I. Soloviev, and M. V. Tereshonok, "Adiabatic superconducting cells for ultra-low-power artificial neural networks," *Beilstein J. Nanotechnol.* **7**, 1397–1403 (2016).
- ⁸N. V. Klenov, A. E. Schegolev, I. I. Soloviev, S. V. Bakurskiy, and M. V. Tereshonok, "Energy efficient superconducting neural networks for high-speed intellectual data processing systems," *IEEE Trans. Appl. Supercond.* **28**, 1–6 (2018).
- ⁹R. Cheng, U. S. Goteti, and M. C. Hamilton, "Spiking neuron circuits using superconducting quantum phase-slip junctions," *J. Appl. Phys.* **124**, 152126 (2018).
- ¹⁰I. I. Soloviev, A. E. Schegolev, N. V. Klenov, S. V. Bakurskiy, M. Y. Kupriyanov, M. V. Tereshonok, A. V. Shadrin, V. S. Stolyarov, and A. A. Golubov, "Adiabatic superconducting artificial neural network: Basic cells," *J. Appl. Phys.* **124**, 152113 (2018).
- ¹¹M. L. Schneider, C. A. Donnelly, S. E. Russek, B. Baek, M. R. Pufall, P. F. Hopkins, P. D. Dresselhaus, S. P. Benz, and W. H. Rippard, "Ultralow power artificial synapses using nanotextured magnetic Josephson junctions," *Sci. Adv.* **4**, e1701329 (2018).
- ¹²M. L. Schneider, C. A. Donnelly, I. W. Haygood, A. Wynn, S. E. Russek, M. A. Castellanos-Beltran, P. D. Dresselhaus, P. F. Hopkins, M. R. Pufall, and W. H. Rippard, "Synaptic weighting in single flux quantum neuromorphic computing," *Sci. Rep.* **10**, 1 (2020).
- ¹³B. Baek, M. L. Schneider, M. R. Pufall, and W. H. Rippard, "Anomalous supercurrent modulation in Josephson junctions with Ni-based barriers," *IEEE Trans. Appl. Supercond.* **28**, 1–5 (2018).
- ¹⁴J. A. Glick, M. A. Khasawneh, B. M. Niedzielski, R. Loloee, W. P. Pratt, N. O. Birge, E. C. Gingrich, P. G. Kotula, and N. Missert, "Critical current oscillations of elliptical Josephson junctions with single-domain ferromagnetic layers," *J. Appl. Phys.* **122**, 133906 (2017).
- ¹⁵I. M. Dayton, T. Sage, E. C. Gingrich, M. G. Loving, T. F. Ambrose, N. P. Siwak, S. Keebaugh, C. Kirby, D. L. Miller, A. Y. Herr, Q. P. Herr, and

- O. Naaman, "Experimental demonstration of a Josephson magnetic memory cell with a programmable φ -junction," *IEEE Magn. Lett.* **9**, 1–5 (2018).
- ¹⁶J. W. A. Robinson, S. Piano, G. Burnell, C. Bell, and M. G. Blamire, "Critical current oscillations in strong ferromagnetic π junctions," *Phys. Rev. Lett.* **97**, 1 (2006).
- ¹⁷V. Aguilar, D. Korucu, J. A. Glick, R. Loloee, W. P. Pratt, and N. O. Birge, "Spin-polarized triplet supercurrent in Josephson junctions with perpendicular ferromagnetic layers," *Phys. Rev. B* **102**, 024518 (2020).
- ¹⁸A. I. Buzdin, "Proximity effects in superconductor-ferromagnet heterostructures," *Rev. Mod. Phys.* **77**, 935 (2005).
- ¹⁹J. Linder and J. W. A. Robinson, "Superconducting spintronics," *Nat. Phys.* **11**, 307–315 (2015).
- ²⁰C. Bell, G. Burnell, C. W. Leung, E. J. Tarte, D.-J. Kang, and M. G. Blamire, "Controllable Josephson current through a pseudospin-valve structure," *Appl. Phys. Lett.* **84**, 1153–1155 (2004).
- ²¹V. V. Ryazanov, V. A. Oboznov, A. Y. Rusanov, A. V. Veretennikov, A. A. Golubov, and J. Aarts, "Coupling of two superconductors through a ferromagnet: Evidence for a π junction," *Phys. Rev. Lett.* **86**, 2427–2430 (2001).
- ²²T. van Duzer and C. W. Turner, *Principles of Superconductive Devices and Circuits* (Elsevier, 1981).
- ²³K. K. Likharev and V. K. Semenov, "RSFQ logic/memory family: A new Josephson-junction technology for digital systems," *IEEE Trans. Appl. Supercond.* **1**, 3–28 (1991).
- ²⁴S. K. Tolpygo and V. K. Semenov, "Increasing integration scale of superconductor electronics beyond one million Josephson junctions," *J. Phys.: Conf. Ser.* **1559**, 012002 (2020).
- ²⁵A. Fischer, R. Kruk, and H. Hahn, "A versatile apparatus for the fine-tuned synthesis of cluster-based materials," *Rev. Sci. Instrum.* **86**, 023304 (2015).
- ²⁶N. Gack, G. Iankevich, C. Benel, R. Kruk, D. Wang, H. Hahn, and T. Reisinger, "Magnetotransport properties of ferromagnetic nanoparticles in a semiconductor matrix studied by precise size-selective cluster ion beam deposition," *Nanomaterials* **10**, 2192 (2020).
- ²⁷V. Ambegaokar and B. I. Halperin, "Voltage due to thermal noise in the dc Josephson effect," *Phys. Rev. Lett.* **22**, 1364–1366 (1969).
- ²⁸Y. M. Ivanchenko and L. A. Zil'berman, "The Josephson effect in small tunnel contacts," *Sov. Phys. JETP* **28**, 1272 (1969).